

Calorimetric and optical microscopic studies on one ferroelectric liquid-crystal compound with the smectic- A^* phase

C. C. Huang and D. S. Lin

School of Physics and Astronomy, University of Minnesota, Minneapolis, Minnesota 55455

J. W. Goodby,* M. A. Waugh, S. M. Stein, and E. Chin

AT&T Bell Laboratories, Murray Hill, New Jersey 07974

(Received 30 June 1989)

Detailed calorimetric measurements have been carried out on the chiral and racemic versions of one chiral liquid-crystal compound that exhibits an unusual and new smectic- A^* ($Sm-A^*$) phase in the pure chiral compound. Both the smectic- A ($Sm-A$)-smectic- C ($Sm-C$) transition in the racemic compound and the $Sm-A^*$ -chiral- $Sm-C$ transition in the pure chiral compound display a first-order transition with heat-capacity anomalies qualitatively similar to but quantitatively different from that observed in the ordinary $Sm-A$ - $Sm-C$ transition. Results from optical microscopic studies on the phase diagram of binary mixtures of the dextro and levo versions of the chiral compounds are reported.

In characterizing new ferroelectric liquid-crystal compounds, recently Goodby *et al.*^{1,2} have discovered and reported a new liquid-crystal mesophase [so-called smectic- A^* ($Sm-A^*$) phase] between the isotropic (I) and chiral smectic- C ($Sm-C^*$) phase among some members of the homologous series *S*- or *R*-1-methylheptyl 4'-[4''-*n*-alkyloxy phenyl] propionoyloxy]-biphenyl-4-carboxylate (*n*P1M7) with long alkyl chain length. Optical and x-ray studies indicate that in the $Sm-A^*$ phase the molecules are arranged in layers with their long axes on average parallel to the layer normal, as in the smectic- A ($Sm-A$) phase. However, in addition to layers, it also has a helical structure with the helical axis propagating in a direction parallel to the layer planes, as shown in Fig. 1. Namely, the $Sm-A$ layering structure is interrupted by liquidlike regions which are supposed to contain numerous defects. Independently, employing the theory of the Abrikosov dislocation lattice in type-II superconductors to the chiral smectic liquid crystal, Renn and Lubensky³ have suggested the existence of the twist-grain-boundary (TGB) phase. The TGB phase consists of a regular array of twist grain boundaries each of which is composed of straight and regularly spaced parallel screw dislocations. The direction of screw dislocations is rotated by a constant angle between adjacent grain boundaries. There exist strong similarities between the observed $Sm-A^*$ phase and the proposed TGB phase, although the regularity of the array of screw dislocations being predicted theoretically has not been established experimentally. To obtain further physical insight into the properties of the intriguing $Sm-A^*$ phase, we have carried out detailed heat-capacity studies on both the chiral and racemic version of the tetradecyloxy compound (14P1M7) in this homologous series. We have also performed optical microscopic studies on the binary mixtures of the dextro and levo versions of this compound. The chemical formula of the compound and transition sequences for the chiral and racemic versions are given in Ref. 4. Normally, additional thermal energy is required to compensate the energy related to the spontaneous polarization and/or destroy the helical pitch order

associated with the $Sm-C^*$ phase. Thus the $Sm-A$ - $Sm-C^*$ transition temperature in the chiral compound is usually higher than the $Sm-A$ - $Sm-C$ transition temperature of the corresponding racemic mixture.⁵ Here a different scenario is obtained. The $Sm-A^*$ - $Sm-C^*$ has about the same (slightly lower) transition temperature as that of the $Sm-A$ - $Sm-C$ in the racemic version of the same compound. This difference is believed to be related to the existence of the $Sm-A^*$ phase instead of the $Sm-A$ phase above the $Sm-C^*$ phase in the chiral compound.

A Zeiss polarizing optical microscope equipped with a

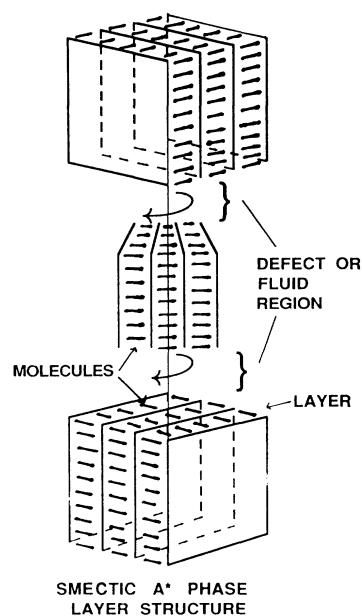


FIG. 1. A pictorial representation of the $Sm-A^*$ phase, adapted from Ref. 1. (Reprinted by permission from Nature Vol. 337, p. 449. Copyright © 1988 Macmillan Magazines, Ltd.)

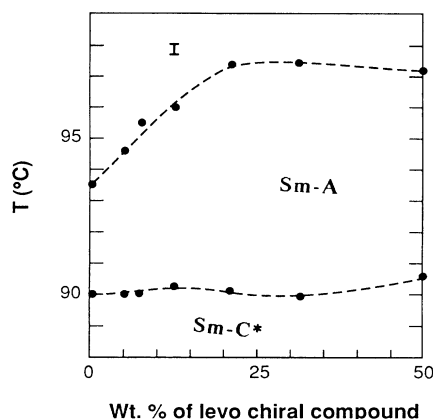


FIG. 2. Temperature-composition phase diagram of the levo in dextro chiral compound. The dashed lines are guides for eyes only.

Mettler hot stage and a 35-mm camera is employed to study the binary phase diagram of the mixtures of the dextro and levo chiral 14P1M7 compounds. The results are displayed in Fig. 2. Below 93.5 °C of the pure dextro chiral compound, a platelet texture shown in Fig. 3(a) characterizes the $Sm-A^*$ phase. Some Grandjean plane textures can be seen in heating from the low-temperature phase. The second texture is similar to that of the cholesteric phase. This indicates that the $Sm-A^*$ phase with a layer structure¹ has a helical structure. The 50%-50% mixture (racemic mixture) displays primarily a homeotropic texture with many and very small islands containing a focal conic texture. Decreasing the concentration of the levo version of the chiral compound in the binary mixture will tend to increase the size of the focal conic domain regions; but, not until the mixture with 15% levo compound, do the focal conic regions become so large and occupy about half of the sample. Figure 3(b) displays the typical focal conic texture for the $Sm-A$ phase obtained from a 12.7%(levo)-87.3%(dextro) mixture. Figures 3(c) and 3(d) show photomicrographs of the 7.5%(levo)-92.5%(dextro) and the 5.0%(levo)-95.0%(dextro) mixtures which exhibit very unique textures below the isotropic phase. Furthermore, the transition temperature into the isotropic phase decreases as the binary mixtures approach the pure chiral compound. While the transition into the $Sm-C$ (or $Sm-C^*$) varies only in a narrow temperature range and remains fairly constant throughout the mixtures, the transition into the isotropic phase makes a very quick drop near the chiral compound. Except in the vicinity of the pure chiral compound, the mixture displays the characteristic $Sm-A$ texture. In the $Sm-A^*$ phase, the existence of the liquidlike region between the $Sm-A$ layering structure is consistent with the fact that $I-Sm-A^*$ transition temperature is lower than the $I-Sm-A$ one. Further investigations are required to address whether the unique textures observed in two mixtures with 7.5%(levo) and 12.7%(levo) signal the change from the $Sm-A$ phase to $Sm-A^*$ one. No sharp boundary or phase transition can be identified to separate the $Sm-A$ phase from the $Sm-A^*$ phase.

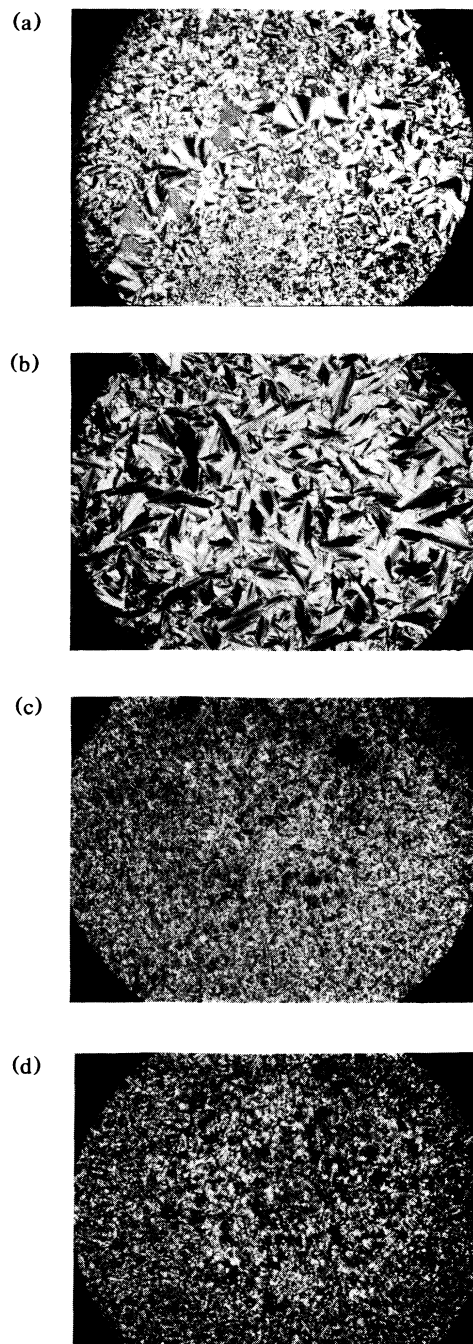


FIG. 3. Photomicrograph of the binary mixtures (a) pure chiral compound at 92.1 °C; (b) 12.7%(levo)-87.3%(dextro) mixture at 95.3 °C; (c) 7.5%(levo)-92.5%(dextro) mixture at 91.6 °C; (d) 5.0%(levo)-95.0%(dextro) mixture at 93.6 °C.

The temperature dependences of heat capacity for the chiral and racemic version are displayed in Figs. 4 and 5, respectively. In the case of the chiral compound, both heating and cooling runs show a large hump on the high-temperature side of a sharp rise in heat capacity at about 367 K. This bump also shows up in the differential scan-

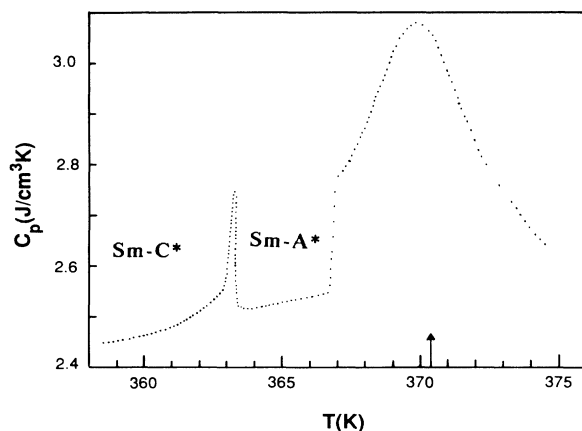


FIG. 4. Heat capacity per unit volume of the pure dextro chiral compound.

ning calorimetry (DSC) measurement.² Polarizing optical microscopic observation on the sample indicates that the sharp rise in the heat capacity at 367 K signals the transition to the isotropic phase and no other feature can be identified corresponding to the broad hump. At this moment, we do not have any explanation for the existence of the wide heat-capacity bump. X-ray data² indicate regions with small Sm-C-like correlations above the Sm-A* phase and optical measurements show optical rotation in this region.⁶ This suggests an amorphous chiral phase reminiscent of the blue phase III, but different because the isotropic to blue phase III transition exhibits a sharp heat-capacity feature associated with a first-order transition.^{7,8}

The heat capacity associated with the Sm-A*-Sm-C* transition shows a sharp rise on the high-temperature side which is similar to the ordinary Sm-A-Sm-C transition. However, a discernible kink exists on the low-temperature side of the heat-capacity anomaly. At the moment, we do not have any model to explain this heat-capacity anomaly. Because the heat-capacity anomaly is not very sharp, determining whether the transition is the first order or by the technique of thermal hysteresis is inconclusive.

A 50%-50% mixture of the dextro and levo version of the chiral compound was prepared to obtain the racemic mixture. Optical microscopic studies on the mixture shows that the transition from the isotropic phase to the Sm-A phase is signaled by very small islands of focal-conic structure in a predominant dark background. Upon further cooling into the Sm-C phase, the schlieren texture shows up. This indicates that the molecules prefer the homeotropic arrangement in the Sm-A phase. The heat-capacity peak associated with the I-Sm-A transition is strongly first order with a much narrower width (≈ 0.3 K) in comparison with the I-Sm-A* transition of the chiral compound. The location of the I-Sm-A transition peak, which is indicated by an arrow in Fig. 4, is about the same as the peak position of the broad peak found in the chiral compound. In principle, it would be nice to compare the heat of transition between the I-Sm-A and I-Sm-A* transitions. However, the ac calorimeter does

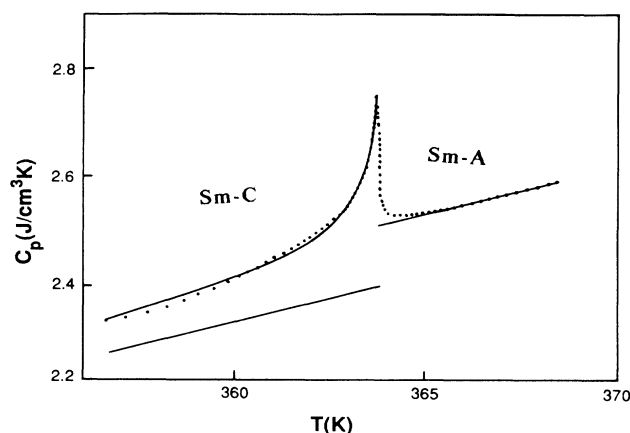


FIG. 5. Heat capacity per unit volume of the racemic mixture. Solid lines are fitted curves. The required background term in the Sm-C phase is shown as a straight line in the low-temperature side.

not produce an accurate measure of the latent heat.

The heat-capacity data in the vicinity of the Sm-A-Sm-C transition are shown in Fig. 5 as dots. Qualitatively, the heat-capacity anomaly is similar to that of the other Sm-A-Sm-C transition. However, if one treats a linear extrapolation of the high-temperature side of data to be the background of the data on the low-temperature side, some of the low-temperature data will be below the background. Consequently, in order to fit the data to an expression derived from an extended mean-field free energy,⁹ a jump in the background heat capacity at the transition temperature is assumed.

The heat-capacity expression derived from the extended mean-field model including the sixth-order term of the order parameter is as follows:⁹

$$C = \begin{cases} B + D(T - T_c), & T > T_c, \\ A(T_m - T)^{-1/2} + B + D(T - T_c), & T < T_c. \end{cases} \quad (1a)$$

Here T_c is the transition temperature. The background term $[B + D(T - T_c)]$ in the heat capacity is obtained from the part of free energy which is not a function of the order parameter; the temperature $T_m = T_c(1 + t_0/3)$. The dimensionless parameter t_0 characterizes the importance of the sixth-order term in the free-energy expansion.⁹ To minimize the number of fitting parameters, we assume that the coefficient D is the same for $T > T_c$ and $T < T_c$ and there exists a jump in the constant background term $[B^+ (T > T_c)$ and $B^- (T < T_c)]$ at T_c . The value of D can be determined from the slope of our experimental data with $T > T_c$. The fitting results are displayed as solid lines in Fig. 5. Overall, Eq. 1(b) gives fairly reasonable fitting to the experimental data. The part of the $[B^- + D(T - T_c)]$ term used in the fitting for $T < T_c$ is shown in Fig. 5. The fitting parameters are $T_m = 363.89$ K, $A = 0.168$ J/cm³K^{1/2}, $B^+ = 2.52$ J/cm³K, $B^- = 2.41$ J/cm³K, $D = 0.0170$ J/cm³K², and $T_c = 363.74$ K, which is chosen to be the midpoint of the mean-field heat-capacity jump.

Compiling all the available high-resolution data near the Sm-*A*-Sm-*C* or Sm-*A*-Sm-*C*^{*} transition, Huang and Lien¹⁰ found that all the existing Sm-*A*-Sm-*C* (or Sm-*C*^{*}) transitions behaved mean-field-like and were continuous and near the mean-field tricritical point. Furthermore, compounds with a smaller Sm-*A* temperature range seem to be closer to the mean-field tricritical point with the mean-field coefficient *b* of the fourth-order term being zero. The existing data suggest that a compound with the Sm-*A*-Sm-*C* transition temperature around 90 °C will be a continuous one provided the temperature range for the Sm-*A* phase is greater than 4.4 K. Here the Sm-*A* phase temperature range for the racemic 14P1M7 is about 6.6 K. Accordingly, we expect that the Sm-*A*-Sm-*C* transition of this compound should be continuous. However, thermal hysteresis of about 10 mK (resolution 4 mK) between the heating and cooling runs was found. The first-order Sm-*A*-Sm-*C* transition is also accompanied by a jump in the background heat capacity at *T*_c. Actually, the heat-capacity data for the chiral compound shown in Fig. 4 exhibit a similar jump. Namely, a linear extrapolation of the heat capacity in the Sm-*A*^{*} phase to the Sm-*C*^{*} phase results in a good portion of heat-capacity data being below the background term.

Recently, in investigating the Sm-*A*-Sm-*C* (or Sm-*C*^{*}) transition of many new chiral liquid-crystal compounds, Liu *et al.*¹¹ have found that the magnitude of the transverse molecular dipole moment plays an important role in determining the nature of the Sm-*A*-Sm-*C* (or Sm-*C*^{*}) transition. In fact, the compounds with large value of the transverse molecular dipole moment favor first-order Sm-*A*-Sm-*C* (or Sm-*C*^{*}) transitions. About 30 K below the Sm-*A*-Sm-*C*^{*} transition temperature, the spontaneous polarization of 14P1M7 reaches approximately 100 nC/cm² (Ref. 2), which is fairly large in comparison with those compounds compiled by Huang and Lien. This suggests that the molecule has a large transverse dipole moment. We believe that this is the major reason why the Sm-*A*-Sm-*C* of this racemic mixture is first order.

The authors would like to thank H. Y. Liu for help in data acquisition and R. Pindak for stimulating discussions. This work is supported in part by the Donors of the Petroleum Research Fund, administered by the American Chemical Society. The equipment for this research work was purchased with the National Science Foundation Grant No. DMR-85-03419.

*Present address: School of Chemistry, The University, Hull HU6 7RX, England.

¹J. W. Goodby, M. A. Waugh, S. M. Stein, E. Chin, R. Pindak, and J. S. Patel, *Nature (London)* **337**, 449 (1988).

²J. W. Goodby, M. A. Waugh, S. M. Stein, E. Chin, R. Pindak, and J. S. Patel (unpublished); R. Pindak, *Bull. Am. Phys. Soc.* **34**, 806 (1989).

³S. R. Renn and T. C. Lubensky, *Phys. Rev. A* **38**, 2132 (1988).

⁴The chemical formula for 14P1M7 is



Transition sequences are *I*(93.5 °C) → Sm-*A*^{*}(90.1 °C)

→ Sm-*C*^{*} for the chiral version and *I*(97.2 °C) → Sm-*A*(90.6 °C) → Sm-*C* for the racemic one.

⁵R. B. Meyer, *Mol. Cryst. Liq. Cryst.* **40**, 33 (1977); S. C. Lien, C. C. Huang, and J. W. Goodby, *Phys. Rev. A* **29**, 1371 (1984).

⁶R. Pindak and M. Marcus (private communication).

⁷R. N. Kleiman, D. J. Bishop, R. Pindak, and P. Taborek, *Phys. Rev. Lett.* **53**, 2137 (1984).

⁸J. Thoen, *Phys. Rev. A* **37**, 1754 (1988).

⁹C. C. Huang and J. M. Viner, *Phys. Rev. A* **25**, 3385 (1982).

¹⁰C. C. Huang and S. C. Lien, *Phys. Rev. A* **31**, 2621 (1985).

¹¹H. Y. Liu, C. C. Huang, T. Min, D. M. Wand, M. D. Walba, N. A. Clark, Ch. Bahr, and G. Heppke (unpublished).

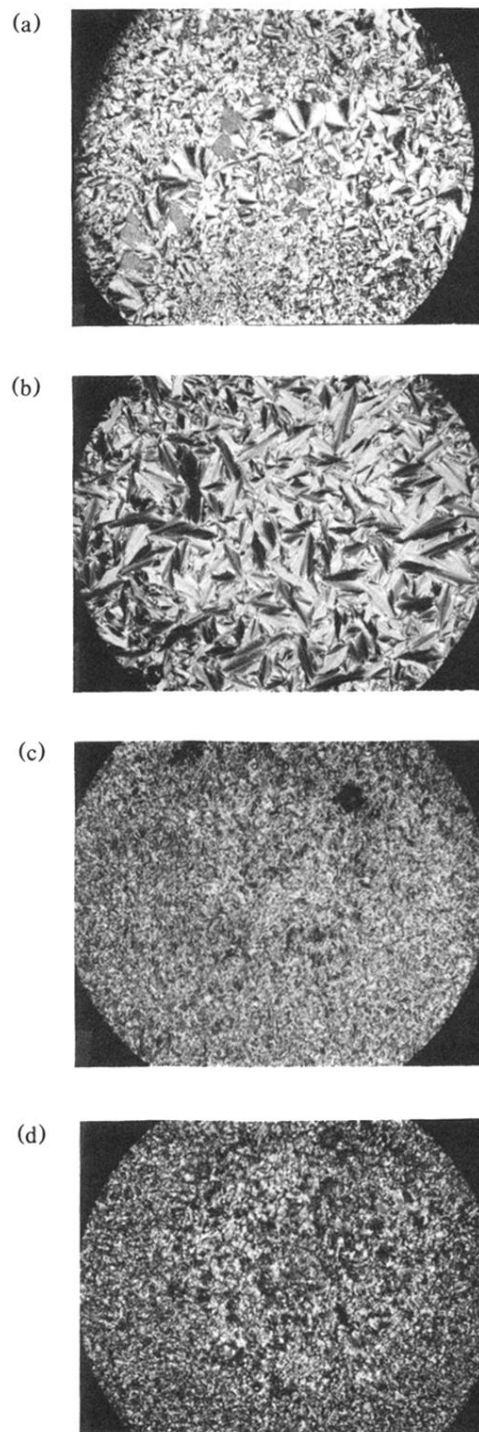


FIG. 3. Photomicrograph of the binary mixtures (a) pure chiral compound at 92.1 °C; (b) 12.7% (levo)-87.3% (dextro) mixture at 95.3 °C; (c) 7.5% (levo)-92.5% (dextro) mixture at 91.6 °C; (d) 5.0% (levo)-95.0% (dextro) mixture at 93.6 °C.